HYBRID PRESSURE CONTROL CONCEPT FOR A SPEED VARIABLE AC MOTOR PUMP IN AEROSPACE APPLICATION

Joerg Engelhardt, Carsten Greissner

Technical University of Hamburg-Harburg, Institute for Aircraft Systems Engineering, Nesspriel 5, 21129 Hamburg, Germany
http://www.tuhh.de/fst
j.engelhardt@tuhh.de, greissner@tuhh.de

Abstract

This paper describes a new pressure control strategy for AC motor driven pumps in aircraft application. Both, swash plate position and pump speed are used for controlling system pressure in a hybrid approach. The requirements for the pressure control loop and the design methods for the hybrid control circuits with a load observer are introduced. The new control concept has been implemented into an experimental set-up. The validation and evaluation of simulation results on the test rig are discussed in detail. Finally, the new hybrid approach is compared to the conventional approach concerning efficiency, noise level and wear for typical aircraft flight missions.

Keywords: Aerospace fluid power systems, AC motor pump, variable speed drives, brushless DC motor, pressure control loop, load observer

1 Introduction

The electric motor driven pumps used in today's commercial aircraft are typically driven by induction motors at constant speed. A hydro-mechanical swash plate compensator is used for pressure control. This design yields the drawback of high speed induced losses and noise emission especially during phases of low consumer activities which are typical for the operation of aircraft hydraulic systems. In practical application, flow demand peaks which require full pump speed occur very seldom, mostly during take-off and landing (see Fig. 1).

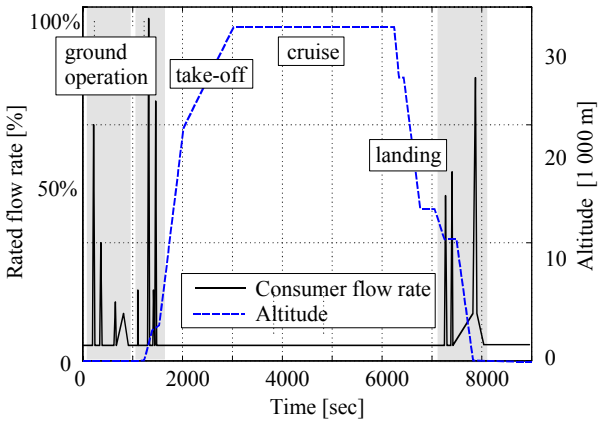

Fig. 1: *Hydraulic load profil of a civil transport aircraft*

A possible approach to resolve this problem would be the usage of fixed displacement pumps with speed controlled AC motors. This solution is established for electrohydrostatic actuators (EHAs) in power-by-wire flight control architectures and could easily be adapted to a pressure control loop. The EHA principle is characterised by natural adaptation of pump speed to consumer flow, but the combination of motor torque and inertia significantly limits the dynamics of speed and pressure control.

Aircraft fluid power systems are typically characterised by rather high requirements for system pressure quality under transient conditions. Thus, the usage of speed controlled fixed displacement pumps appears to not be feasible with existing AC drives.

Consequently, this contribution presents a hybrid approach using a speed controlled brushless DC motor for driving the pump and a digital swash plate and pressure control loop (Fig. 2). Both, speed and swash plate are used for controlling system pressure. This approach combines the excellent dynamics of pure swash plate control with the power optimised operation of speed controlled fixed displacement pumps.

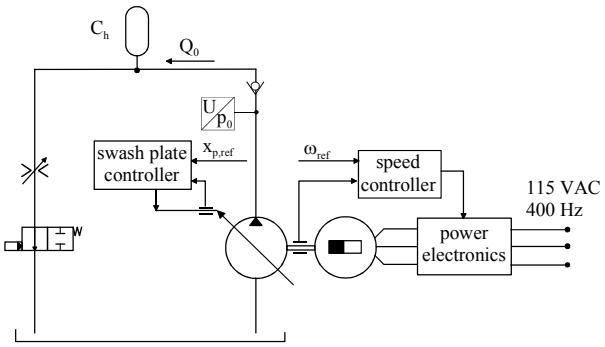

Fig. 2*: Principle concept of an AC motor pump with a brushless DC servo drive*

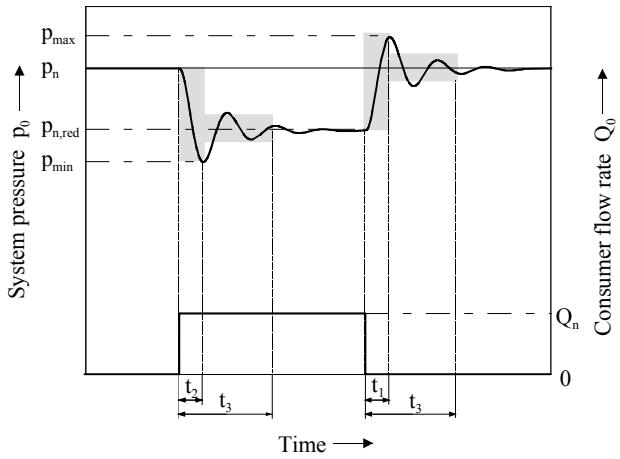

Fig. 3: *Requirements for pump response*

2 Requirements for aerospace pumps

Dynamic requirements for aerospace hydraulic pumps are typically defined in time domain according to the military specification MIL-P-19692E (1994). Figure 3 shows the required response of the systems pressure resulting from a step input in system flow rate Q_0. System pressure must be kept within the indicated areas characterised by the response times t_1, t_2 and t_3 and the pressure limits p_{max}, p_{min} and $p_{n,red}$ for a change from full flow to zero flow and vice versa. Respective data for a 3000 psi system is given in Table 1. The MIL-specification does not explicitly define the minimum transient pressure p_{min}. Therefore, a symmetrical behaviour is assumed for the controller design process.

Table 1: Performance requirements (MIL-P-19692E)

Nominal system pressure p_n	206 (3000	bar psi)
Reference gradient $\dot{p}_0$	3450 (5000	bar/sec psi/sec)
Rated flow rate Q_n	70	l/min
Reference capacity C_h	$3.38 \cdot 10^{-12}$	m^3/Pa
Max. transient pressure p_{max} (rel.)	135 % p_N	-
Max. transient pressure p_{max} (abs.)	278 (4030	bar psi)
Min. transient pressure p_{min} (rel.)	65 % p_N	-
Min. transient pressure p_{min} (abs.)	134 (1940	bar psi)

Pump performance has to be demonstrated in a reference system depending on pump size. When the system flow is suddenly reduced from rated flow Q_n to zero, a rate of pump discharge pressure $\dot{p}_{0,ref}$ of 345000 kPa/sec shall occur in the test circuit. Thus, the hydraulic reference capacity C_h yields:

$$C_h = \frac{Q_n}{\dot{p}_{0,ref}} \quad . \tag{1}$$

3 System model

3.1 Non-linear system model

The AC motor pump can be described by the following set of non-linear differential equations for the variable displacement hydraulic pump (Backé, 1992) and the brushless DC motor (Schröder, 1994).

For analysing the permanent magnet synchronous motor, a 2-phase equivalent circuit model is used (Park, 1933). The stator and space fixed 3-phase variables for flux and voltage are transformed into a rotating, rotor fixed d-q-frame.

The d- and q-axis voltage equations are given by :

$$\begin{aligned} \frac{d\,\Psi_d}{dt} &= u_d - R_l\, i_d + \omega_{el}\, \Psi_q \\ \frac{d\,\Psi_q}{dt} &= u_q - R_l\, i_q + \omega_{el}\, \Psi_d \end{aligned} \tag{2}$$

with the flux linkage equations:

$$\begin{aligned} \Psi_d &= L_d\, i_d + \Psi_{pm} \\ \Psi_q &= L_q\, i_q \quad . \end{aligned} \tag{3}$$

Motor torque can be expressed as:

$$M_{Mi} = \frac{3}{2} Z_p \left(\Psi_{pm}\, i_q + \left(L_d - L_q \right) i_d\, i_q \right) \quad . \tag{4}$$

Flow delivery of the pump can be represented as:

$$Q_p = Q_{p,th} - Q_{dis} \tag{5}$$

with the theoretical pump flow $Q_{p,th}$ given by:

$$Q_{p,th} = \frac{V_{max}\, \omega_{mech}}{2\pi} \frac{x_p}{x_{p,max}} \, . \tag{6}$$

and the volumetric pump losses Q_{dis}.

The swash plate actuator position x_p can be derived from servo valve flow Q_{sv} and piston area A_p:

$$\frac{d\,x_p}{dt} = \frac{Q_{sv}}{A_p} \tag{7}$$

with servo valve flow assumed to be a linear function of the servo valve position y_{sv}:

$$Q_{sv} = c_Q \; y_{sv} \quad . \tag{8}$$

The dynamic response of the servo valve is modelled as a second order system with the servo valve current i_{sv} as input:

$$\frac{d^2 y_{sv}}{dt^2} = -2D_{sv}\omega_{sv}\frac{d\,y_{sv}}{dt} - \omega^2{}_{sv}\, y_{sv} + k_{sv}\omega^2{}_{sv} \cdot i_{sv} \tag{9}$$

with

$$k_{sv} = \frac{y_{sv}}{i_{sv}} \quad . \tag{10}$$

The torque which is required to drive the pump depends on pump flow and pressure (hydraulic torque) and on friction losses:

$$M_p = M_{hyd} + M_{fric,p} \tag{11}$$

with the hydraulic torque

$$M_{hyd} = \frac{(p_0 - p_r)V_{max}}{2\pi}\frac{x_p}{x_{p,max}} . \tag{12}$$

Hence, the equation of motion for the whole system results in:

$$J_{total}\frac{d\,\omega_{mech}}{dt} = M_{Mi} - M_p - M_{fric,m} \quad . \tag{13}$$

The system pressure p_0 is calculated from:

$$\dot{p}_0 = \frac{1}{C_h}(Q_p - Q_{load}) \quad . \tag{14}$$

3.2 Linear system model

The equations above are characterised by several non-linearities:

- Swash plate actuator position x_p and servo valve position y_{sv} are mechanically limited.
- Motor current i_q is limited as well.
- Volumetric and torque losses very much depend on operation parameters such as temperature, discharge pressure, flow rate and pump speed.
- d- and q-axis of the brushless DC motor are cross-coupled.
- Saturation effects occur in the brushless DC motor during high phase currents.
- Pump flow rate is non-linear coupled with motor speed by multiplication.
- Hydraulic torque is derived from the product of pressure and swash plate position.

For controller design, the complete model is splitted into the speed control loop of the brushless DC motor and the stand-alone pressure control loop of the hydraulic pump.

For linearisation of the speed control loop, the d-axis of the motor can be neglected because a vector flux control with $i_{d,ref} = 0 \approx i_d$ is applied (Leonhard 1995). Saturation effects are not considered. Friction losses of the pump and the motor are reduced to a common speed depending friction torque with:

$$M_{fric} = M_{fric,p} + M_{fric,m} = c_{fric}\omega_{mech} \quad . \tag{15}$$

Linearisation of the pressure control loop requires to neglect all mechanical limitations. Volumetric losses are reduced to a pressure proportional flow loss:

$$Q_{dis} = c_{le,p0} \cdot p_0 \quad . \tag{16}$$

The pump speed is assumed to remain constant for controller design and the limitation of the motor current is neglected. Figure 4 and 5 show the linear block diagrams of both control loops, respectively.

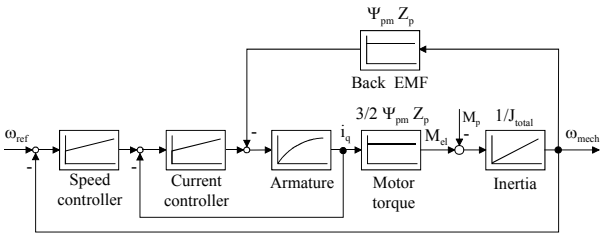

Fig. 4: *Linear speed control loop*

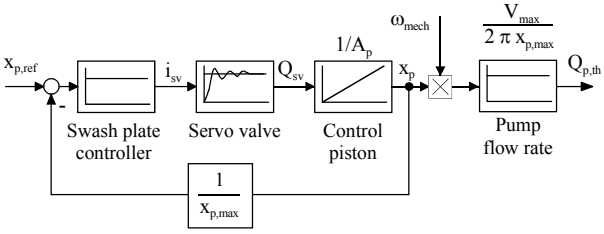

Fig. 5: *Linear swash plate control loop*

4 Hybrid controller design

4.1 Control Strategy

The investigated AC motor pump combines a brushless DC motor and a variable displacement pump with electrohydrostatic swash plate control. In the hybrid pressure control concept, both motor speed and swash plate are used for controlling system pressure (see Fig.6).

The primary pressure controller is a conventional PI control loop, working autonomously by adapting swash plate position to consumer flow.

For adapting pump speed to the actual consumer flow without any additional sensors a load observer is used. During phases of low consumer activities the pump speed is reduced to a minimum level. When a flow demand occurs, the speed increases up to the nominal value of the unit. The acceleration from minimum to nominal speed during an excessive flow demand is the critical case for controller design. Hence, the minimum speed level is determined by the required pressure quality.

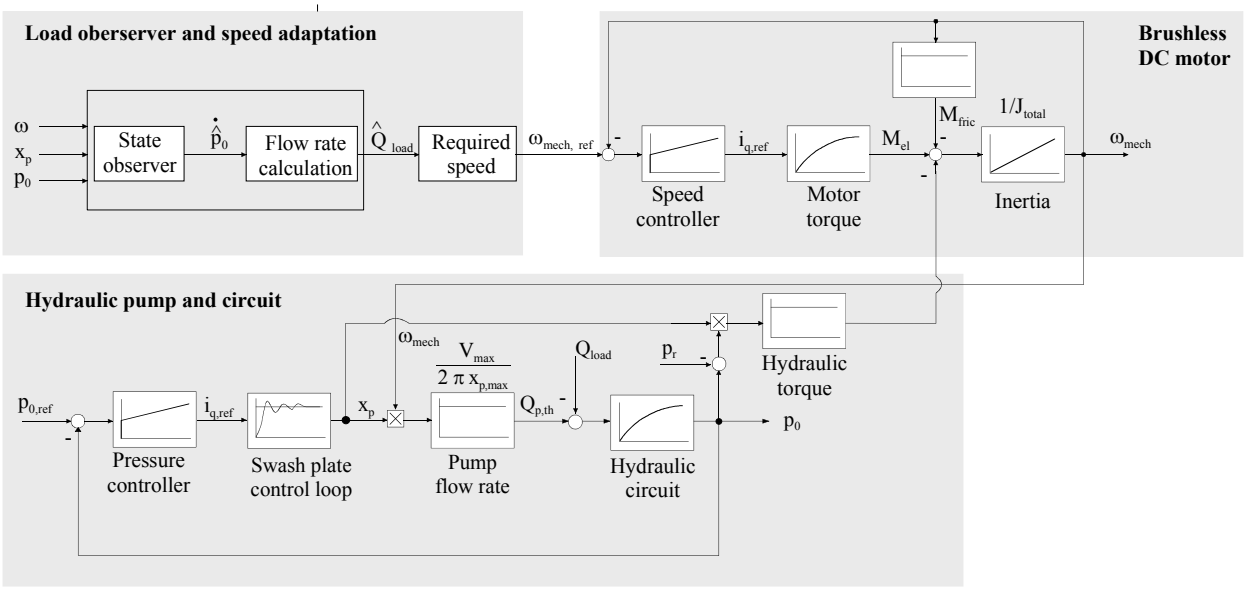

Fig. 6: *Hybrid pressure control loop*

Motamed (1995,1997) has already introduced a similar approach with converter-fed induction drive and a speed stepping technique based on measuring system pressure. In the concept presented here, pump speed is matched directly to consumer flow. Thus offering a more dynamic system performance.

The design of the hybrid controller is devided into three sections:

- the design of the primary pressure controller at nominal speed,
- the strategy for speed adaptation and
- the design of the speed control loop.

4.2 Design of the primary pressure controller

The design process for the primary pressure controller is based on the following assumptions:

- a cascaded loop with PI pressure controller is used
- requirements are defined in time domain as step responses and aim at disturbance rejection
- the dynamic behavior of the swash plate control loop and the current built-up can be neglected

With the assumptions above, the disturbance transfer function is given by

$$G_{\mathrm{d}}(s) = \frac{-\dfrac{1}{C_{\mathrm{h}} p_{\mathrm{n}}} \cdot s}{s^2 + \dfrac{c_{\mathrm{le},p_0} + \gamma\, k_{\mathrm{P},p_0}}{C_{\mathrm{h}}} \cdot s + \dfrac{\gamma\, k_{\mathrm{I},p_0}}{C_{\mathrm{h}}}} \tag{17}$$

with

$$\gamma = \frac{\omega_{\mathrm{n}}\, V_{\max}}{2\,\pi\, p_{\mathrm{n}}} \quad . \tag{18}$$

For

$$k_{\mathrm{I},p_0} \le \frac{\left(c_{\mathrm{le},p_0} + \gamma\, k_{\mathrm{P},p_0}\right)^2}{4\,\gamma\, C_{\mathrm{h}}} \tag{19}$$

the poles s_1 and s_2 are real and no oscillation occur in the step response of the disturbance transfer function.

With real poles, the step response could be computed in time domain by inverse Laplace transformation. The investigation shows the dependence of peak overshoot, peak time and control error after 1 sec on root locus. This dependence is given by the following equations:

$$e_{\mathrm{m}} = \frac{k_{\mathrm{d}}\, Q_{\mathrm{n}}}{s_1 - s_2}\left[\left(\frac{s_1}{s_2}\right)^{\frac{s_1}{s_2 - s_1}} - \left(\frac{s_1}{s_2}\right)^{\frac{s_2}{s_2 - s_1}}\right]$$

$$t_{\mathrm{m}} = \frac{\ln\left(\dfrac{s_1}{s_2}\right)}{s_2 - s_1} \tag{20}$$

$$h_{\mathrm{d}}(t = 1\mathrm{sec}) = k_{\mathrm{d}}\, Q_{\mathrm{n}}\, \frac{e^{s_1} - e^{s_2}}{s_1 - s_2}$$

with

$$k_{\mathrm{d}} = -\frac{1}{C_{\mathrm{h}}\, p_{\mathrm{n}}} \quad . \tag{21}$$

This system of nonlinear equations cannot be solved analytically. Thus, the equations have to be standardized in order to solve this system numerically:

$$\frac{e_{\mathrm{m}}}{k_{\mathrm{d}}\, Q_{\mathrm{n}}} = \frac{1}{s_1 - s_2}\left[\left(\frac{s_1}{s_2}\right)^{\frac{s_1}{s_2 - s_1}} - \left(\frac{s_1}{s_2}\right)^{\frac{s_2}{s_2 - s_1}}\right] \tag{22}$$

$$t_{\mathrm{m}} = \frac{\ln\left(\frac{s_1}{s_2}\right)}{s_2 - s_1} \tag{23}$$

$$\frac{h_{\mathrm{d}}\left(t = 1\mathrm{sec}\right)}{k_{\mathrm{d}}\ Q_{\mathrm{n}}} = \frac{e^{s_1} - e^{s_2}}{s_1 - s_2} \quad . \tag{24}$$

The standardized equations (22) – (24) are universally valid because they only depend on the poles s_1 and s_2. In Fig.7, 8 and 9 peak overshoot , peak time and control error after 1 sec are plotted against root locus.

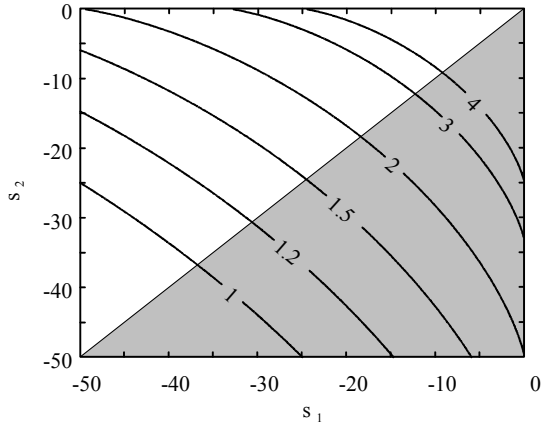

Fig. 7: *Dependence of peak overshoot $e_{\mathrm{m}}/(k_{\mathrm{d}}Q_{\mathrm{n}})$ in % sec on root locus*

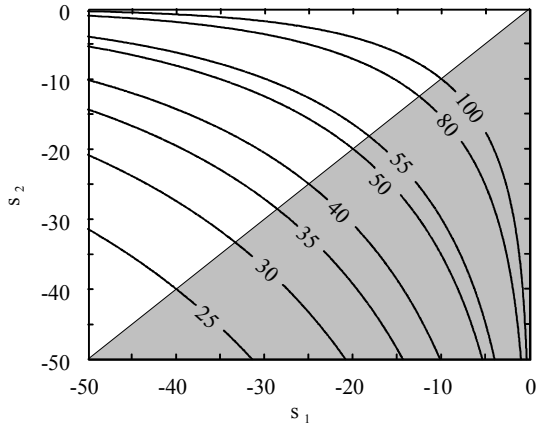

Fig. 8: *Dependence of peak time t_{m} in* ms *on root locus*

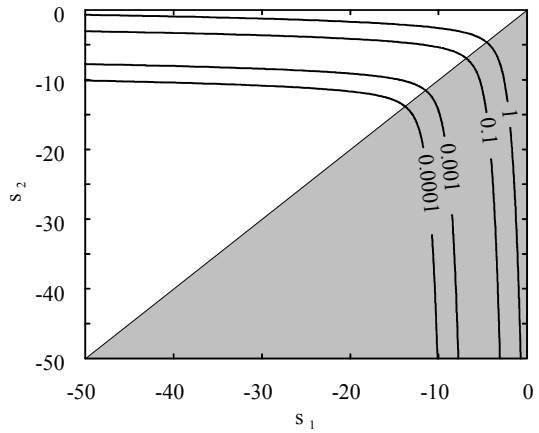

Fig. 9: *Dependence of control error $h_{\mathrm{d}}(t$=1sec$)/(k_{\mathrm{d}}Q_{\mathrm{n}})$ in* % sec *on root locus*

Starting from requirements in time domain given in section 2, Fig. 7, 8 and 9 allow to choose poles s_1 and s_2 which fulfil the given requirements. With the selected poles s_1 and s_2 the coefficients for the PI pressure control loop can be computed from:

$$\begin{aligned} k_{\mathrm{P,p0}} &= -\,2\,\pi\,p_{\mathrm{n}}\,\frac{c_{\mathrm{le,p0}} + C_{\mathrm{h}}\,\left(s_1 + s_2\right)}{\omega_{\mathrm{n}}\,V_{\max}} \\ k_{\mathrm{I,p0}} &= \frac{2\,\pi\,p_{\mathrm{n}}\,C_{\mathrm{h}}\,s_1\,s_2}{\omega_{\mathrm{n}}\,V_{\max}} \quad . \end{aligned} \tag{25}$$

4.3 Load observer

To determine consumer flow Q_{load} without an additional sensor a load observer is used which is described by the following set of equations. The calculation of Q_{load} is based on a state observer for $\dot{p}_0$:

$$\begin{aligned} \dot{\hat{p}}_0 &= \left(p_0 - \hat{p}_0\right) k_{\mathrm{P}} - \frac{c_{\mathrm{le,p_0}}}{C_{\mathrm{h}}}\,\hat{p}_0 + \frac{a}{C_{\mathrm{h}}} + \frac{Q_{\mathrm{p,th}}}{C_{\mathrm{h}}} \\ \dot{a} &= \left(p_0 - \hat{p}_0\right) C_{\mathrm{h}} k_{\mathrm{I}} \quad . \end{aligned} \tag{26}$$

With the observed pressure gradient $\dot{\hat{p}}_0$ the consumer load Q_{load} can be computed from:

$$Q_{\mathrm{load}} = Q_{\mathrm{p,th}} - c_{\mathrm{le,p_0}}\ p_0 - \dot{\hat{p}}_0\ C_{\mathrm{h}} \quad . \tag{27}$$

Although the leakage coefficient $c_{\mathrm{le,p_0}}$ and the system capacity C_{h} are used for the calculation, investigations have shown that the observer itself is robust against parameter variations and uncertainties.

Alternatively, the pressure gradient can directly be computed from the measured pressure signal p_0 by numerical differentiation. But due to the pressure ripple and other noise effects, this approach requires comprehensive filtering. Therefore, here the observer has been chosen for estimating the actual consumer flow.

4.4 Motor speed setting

With notice of consumer and leakage flow, it becomes possible to calculate pump speed command matching the actual consumer flow:

$$\omega_{\mathrm{mech,ref}} = \frac{\omega_{\mathrm{n}}}{Q_{\mathrm{n}}}\left(Q_{\mathrm{load}} + Q_{\mathrm{dis}}\right) \quad . \tag{28}$$

The reference speed is limited by the nominal pump speed and by a lower limit which determines pressure drop during transient load conditions:

$$\omega_{\min} \le \omega_{\mathrm{mech,ref}} \le \omega_{\mathrm{n}} \quad . \tag{29}$$

A rising consumer flow leads directly to an increase in pump speed. On the other hand, the motor does not immediately follow a reduced flow rate. After a latency t_{rest} the controller allows a reduction of pump speed if applicable. Hence, t_{rest} specifies the minimum time period between two acceleration cycles with maximum torque. The introduction of the latency t_{rest} yields three major advantages:

- Pump operation becomes smoother during oscillating loads.
- The defined time period between applying maximum motor torque for acceleration reduces the requirements for motor design.
- The pressure and speed control loop are decoupled, avoiding the risk of non-linear instabilities.

The critical case for the pressure control loop is a flow demand of Q_n occurring when the pump is running at minimum speed. Because of the various non-linearities which characterise the system it is not possible to describe system's behaviour analytically. The minimum speed level must be computed using the non-linear simulation model.

4.5 Speed controller

The brushless DC motor and the power electronics must be able to deliver a continuous torque which evens out the hydraulic torque M_p. For intermittent operations, an additional torque ΔM is needed for acceleration. This available acceleration torque ΔM very much dominates the minimum speed.

The speed controller must be able to follow the commanded speed signal dynamically. A minimum requirement for the speed control loop is to follow the maximum possible rise rate given by the maximum motor torque and inertia. As long as this requirement is fulfilled, control parameter setting has minor influence on system pressure transients. Peak overshoot should be limited to an acceptable level.

5 Experimental validation

The simulation models have been validated on an experimental set-up with a servo drive and an axial piston pump from industrial application (Fig. 10). The test unit is designed for a nominal flow rate Q_n of 70 ltr/min at 206 bar (3000 psi). Both machines are coupled with a shaft, measuring torque and speed. This results in an additional moment of inertia, not present in a prototype model where hydraulic an electrical machine are directly coupled.

The hydraulic capacity of the test circuit has been modified to meet the requirements for a MIL-P-19692E reference system. Consumer flow is simulated with a solenoid valve and a manually adjusted orifice.

The permanent magnet motor is equipped with a water cooling system. Unlike in an aircraft electrical power system (115 VAC, 400 Hz), the servo drive is supplied with 230VAC, 50Hz from the public power supply. Thus, working with a DC link voltage of 600 VDC, not 270 VDC like in an aircraft.

The hybrid pressure control loop is tested with several minimum speed levels ω_{min} for speed adaptation (Fig. 11 and Fig. 12). The test cycle starts with the pump running at minimum speed level ω_{min}. At $t=0.5$ sec a sudden change in consumer flow Q_0 is applied. Simultaneously, speed and pump displacement increase to cope with the drop in system pressure. At $t=1.5$ sec system flow is stopped. Here, only the swash plate is responsible for pressure control. The reduction of speed is not plotted due to the latency t_{rest}. In general, a good conformance between measurement and simulation is achieved with the described non-linear model.

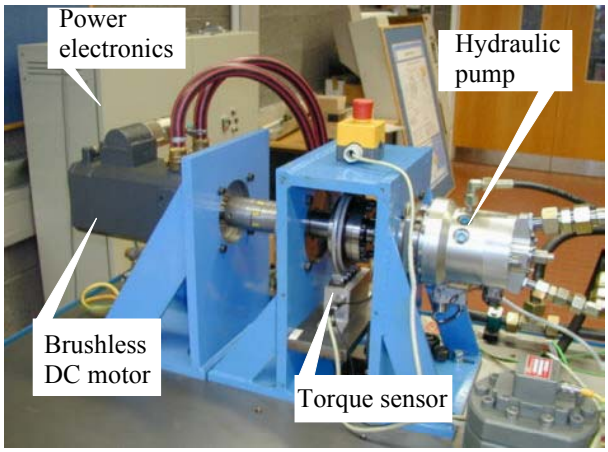

Fig. 10: *AC motor pump test rig*

For $\omega_{min} = 325$ rad/sec (62% of nominal system speed $\omega_n = 524$ rad/sec), the pressure control fulfils all requirements according to MIL-P-19692E indicated by the gray sections. Whereas, reducing ω_{min} below 270 rad/sec yields in a pressure drop below 65% of nominal system pressure (165 bar) when applying the load step to the test circuit.

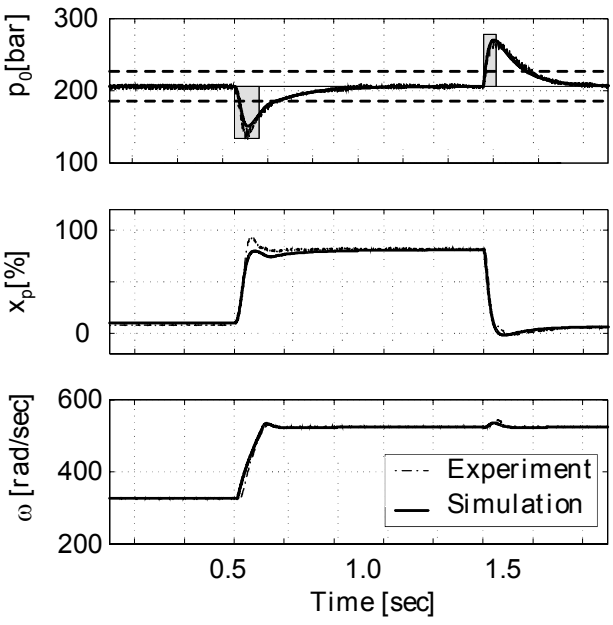

Fig. 11: *Comparison of experiment and simulation with a minimum speed* $\omega_{min} = 325$ rad/sec

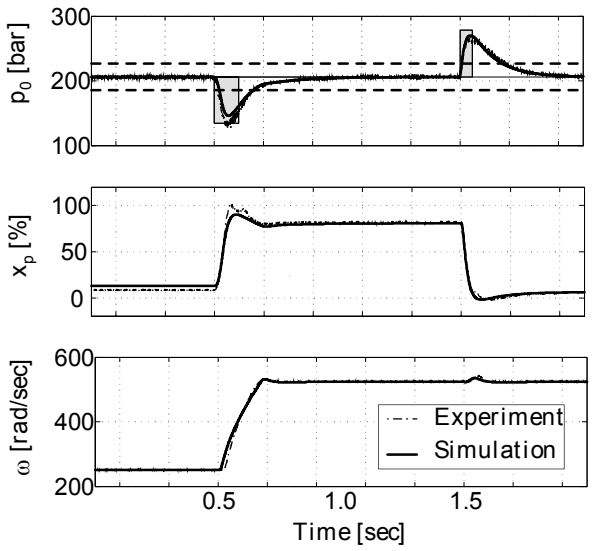

Fig. 12: *Comparison of experiment and simulation with a minimum speed* $\omega_{\min} = 250$ rad/sec

Figure 13 summarizes the maximum pressure drop $p_{\min}$ as a function of mimimum speed level $\omega_{\min}$. A comparision between simuation and experimental results show that the pressure drop in the test rig is more significant than predicted by the model. Nevertheless, a speed reduction during no-load operation of about 50% can be achieved with the experimental set-up.

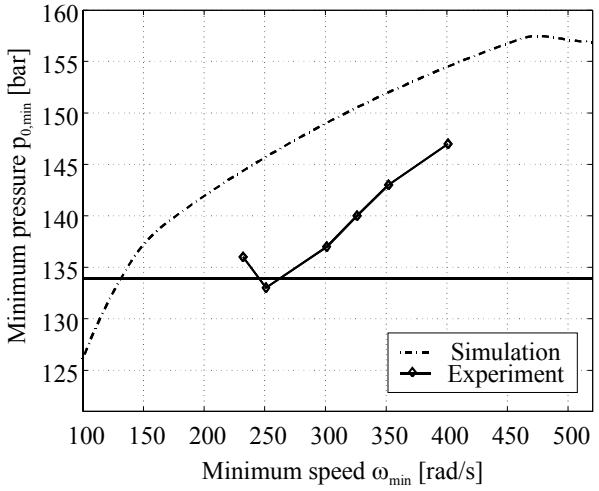

Fig. 13: *Dependence of the minimum pressure on the minimum speed*

6 Evaluation of hybrid controller concept

Today's AC motor pumps are typically driven by induction motors at constant speed. A hydro-mechanical swash plate compensator is used for pressure control. Whereas the pump presented in this paper incorporates an electric servo drive and an axial piston pump with electro-hydrostatic controlled displacement. Hence, the main disadvantages of the new concept are:

- more complex and expensive equipment required
- weight penalties due to the additional power electronics
- reduced reliability mainly due to the complexity of the electronic components

The above mentioned items are less relevant for future aircraft with variable frequency electrical power systems (Bonenfant, 1998). These systems require, per se, the usage of electronically commutated electrical motors to decouple the drive systems from the varying networks frequency. Thus, including all characteristics of the hardware concept described in this paper.

The main advantages of the control strategy presented herewith derive from the reduction of speed during phases of low consumer activities. Experimental tests show a possible reduction of speed of up to 50% without a significant reduction in pressure control quality. Reducing pump speed in general yields the following benefits:

- The noise emission of the experimental set-up has been reduced by approximately 5 db(A).
- Mechanically wear, especially of the hydraulic unit, decreases when reducing speed (Schweitzer et al., 1998; Halat et al., 1998). A higher life cycle can be expected.
- Power losses of the motor pump significantly increase with speed due to viscous friction effect. Adaptation of speed during low-activity periods, reduces the electrical power consumption of the pump and the heat load for the hydraulic power system. Based on the typical profile shown in Fig. 1, a flight mission is simulated with different levels of speed adaptation $\omega_{\min}$. Excepts for very small value of $\omega_{\min}$, a nearly linear reduction of energy losses can be stated (Fig. 14).

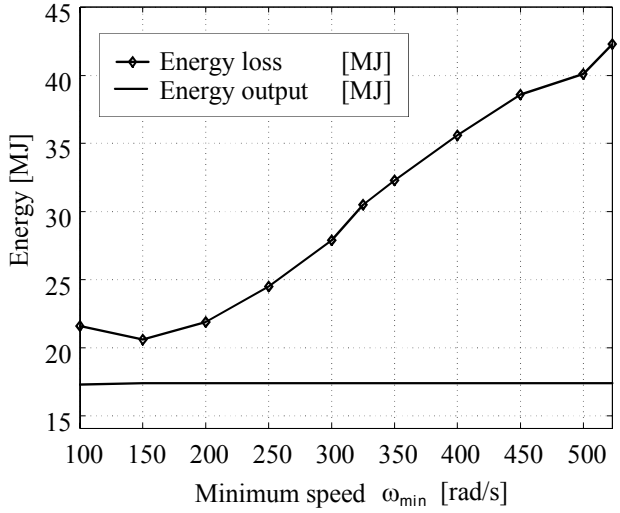

Fig. 14: *Dependence of the energy losses on the choice of minimum speed*

7 Conclusion

This paper presents a new control strategy for AC motor pumps in aerospace application. The concept is based on a set-up with a brushless DC servo drive and a variable displacement pump. Being more complex than today's AC motor pumps, future aircraft power systems with variable electrical frequency will demand very similar set-ups. Thus, for future application adequate hardware will be available.

With this hardware concept, a new control strategy for pressure control has been developed and successfully tested. Main benefit of the proposed controller is the adaptation of pump speed to consumer flow without any significant drawback in pressure quality and without additional sensors. A speed reduction of 50% could be demonstrated, resulting approximately in a 40% decrease in power loss. Naturally, these benefits only become relevant in hydraulic systems with significant phases of low consumer activity.

The effects of transferring the concept on a prototype unit designed for an aircraft environment (reduced inertia, reduced voltage level) will have to be investigated.

For aircraft application, the most important benefits are the reduced thermal load for the hydraulic circuit and the decrease in pump noise. For industrial application, the reduced electrical power consumption itself might also be of great interest.

Further investigations will aim at the network power system quality in terms of voltage distortion due to the use of nonlinear electrical loads such as electronically commutated motors. Especially in isolated electrical power systems, like in commercial aircraft, where power feeder impedance is comparable to that of the generator, excessive harmonics could have adverse effect on the operation of the whole system.

Nomenclature

a	state of observer
A_p	piston area
c_fric	coefficient of total friction
C_h	hydraulic capacity
$c_\mathrm{le,p0}$	leakage coefficient of pump
c_Q	reinforcement of flow rate
D_sv	damping of servo valve
e_m	peak overshoot
$G_\mathrm{d}(s)$	transfer function of disturbance
$h_\mathrm{d}(t)$	disturbance step response
i	current in one branch
J_total	total inertia
k_d	static reinforcement
k_I	integral part of load observer feedback
$k_\mathrm{I,p0}$	integral part of pressure controller
k_P	proportional part of load observer feedback
$k_\mathrm{P,p0}$	proportional part of pressure controller
k_sv	current reinforcement of servo valve
L	inductivity
M_fric	total friction torque
$M_\mathrm{fric,p}$	friction torque of pump
$M_\mathrm{fric,m}$	friction torque of motor
M_hyd	hydraulic torque
M_MI	air gap torque
M_P	total torque of pump
p_0	system pressure
p_max	maximum system pressure
p_min	minimum system pressure
p_n	nominal pressure
$p_\mathrm{n,red}$	reduced nominal pressure
p_r	return pressure
Q_dis	flow rate losses
Q_load	load flow rate
Q_n	nominal flow rate
Q_p	effective flow rate of pump
$Q_\mathrm{p,th}$	theoretical flow rate of pump
Q_sv	flow rate of servo valve
R_l	resistance of stator winding
s	Laplace variable
T_m	peak time
t_rest	time delay
u	voltage across one branch
V_max	displacement volume
x_p	piston position
y_sv	position of spool rod
Z_p	number of pairs of poles
ω_el	electrical angular speed
ω_mech	mechanical angular speed
ω_sv	natural angular frequency of servo valve
Ψ	flux
Ψ_pm	flux of permanent magnet in the stator
	all variables are defined in SI-units
$(\cdot)_\mathrm{d}$	branch d in d-q-frame
$(\cdot)_\mathrm{q}$	branch q in d-q-frame
$(\cdot)_\mathrm{ref}$	set-point
$(\hat{\cdot})$	observer state

References

Backé, W. 1992. *Servohydraulik.* Lecture notes: Institut für hydraulische und pneumatische Antriebe und Steuerungen, RWTH Aachen, Germany.

Bonenfant, L. 1998. *Modélisation et simulation du réseau électrique d'un avion -- Application aux Airbus A330, A340 et A3XX*. Ph.D. Theses, L'Institut National Polytechnique de Toulouse, Laboratoire d'Electrotechnique et d'Electronique de l'ENSEEIHT

Halat, J.A.; Galloway P.W. 1998. *High Pressure Hydraulic Pumps*. Recent Advances in Aerospace Hydraulics, November 24-25 1998, Toulouse

Leonhard, W. 1995. *Control of Electrical Drives*. Springer-Verlag Berlin, Heidelberg, New York

Motamed, F. 1995. *Use of a variable frequency motor controller to drive AC motor pumps on aircraft hydraulic systems*. IECEC - Intersociety Energy Conversion Engineering Conference 1995, American Society of Mechanical Engineers (ASME)

Motamed, F. 1997. *Variable-frequency AC induction motor controller*. Martin Marietta Corp., US Patent, US5668457

MIL-P-19692E *1994.* General Specification for Variable Flow Hydraulic Pumps. *US Department of Defence*

Park, R.H. 1933. *Two reaction theory of synchronous machines: Part II*. AIEE Transactions, Vol. 52, pp.352-355, June 1933

Schröder, D. 2000. *Elektrische Antriebe - Grundlagen*. Springer-Verlag Berlin, Heidelberg, New York

Schweitzer, J.J.; Barrow, G. *1998.* Reliability and Service Experience of Aerospace Hydraulic Rotating. *Recent Advances in Aerospace Hydraulics, November 24-25 1998, Toulouse*

Joerg Engelhardt
Born on December 24th 1970 in Stade (Germany). Study of Mechanical Engineering at the Technical University Hamburg-Harburg (TUHH).

Scientific Employee at the Institute for Aircraft Systems Engineering at the Technical University of Hamburg-Harburg. Specialised on electric and hydraulic power generation and drive technologies in civil aircraft.

Carsten Greissner
Born on November 25th 1975 in Hamburg (Germany). Study of Mechatronics at the Technical University Hamburg-Harburg (TUHH).

Diploma Thesis at the Institute for Aircraft Systems Engineering at the Technical University of Hamburg-Harburg. Scientific Employee at the Institute for Aircraft Systems Engineering at the Technical University of Hamburg-Harburg.